



Real Time Monitoring of the 3D Printing Process

Virginia Engineering Governor's School

Summer 2016

Jaspreet Ranjit

William Makinen



Table of Contents

| | |
|--|-----------|
| Abstract | 2 |
| 1. Introduction | 2 |
| 1.1 Load Sensing Theory | 3 |
| 1.2 Thermometer Theory | 3 |
| 1.3 Profilometer Theory | 4 |
| 2. Previous Work | 4 |
| 2.1 Spectral Graph Theory | 4 |
| 2.2 Heterogeneous Sensors | 5 |
| 3. Experiment Design | 5 |
| 3.1 Load Sensing..... | 5 |
| 3.1.1 Experimental Design | 5 |
| 3.1.2 Sensor Setup | 6 |
| 3.2 Thermometer | 7 |
| 3.2.1 Experimental Design | 7 |
| 3.2.2 Sensor Setup | 7 |
| 3.3 Profilometer..... | 8 |
| 3.3.1 Experimental Design | 8 |
| 3.3.2 Sensor Setup | 8 |
| 4. Data Collection and Analysis | 8 |
| 4.1 Load Sensing..... | 8 |
| 4.2 Thermometer | 9 |
| 4.3 Profilometer..... | 11 |
| 5. Future Directions | 13 |
| Acknowledgements | 14 |
| Figures | 15 |
| Works Cited | 26 |

Abstract

Additive manufacturing (AM) processes such as Fused Filament Fabrication (FFF) are used by 3D printers allow for the rapid small-scale production of dimensionally complex components. However, most 3D printers do not have the required sensors to monitor their production process as it takes pace. This lack of monitoring is the primary reason 3D printing tends to be less reliable than conventional manufacturing methods for the production of consistently precise components. One of the main advantages of installing in-situ sensors in a 3D printer is that the additional data will allow for the detection of build errors early on in the production process as they happen, saving both time and resources. The study presented in this paper explored how the use of a load monitor, a noncontact IR temperature sensor, and a profilometer can monitor various aspects of the printing process in real time, and how this data can be used to ensure the quality and dimensional integrity of a given 3D-printed component. The installation of these sensors produced data that was analyzed for trends to produce parameters from which defects and discrepancies can be detected.

1. Introduction

In recent years, AM techniques such as FFF used by 3D printers have increased exponentially in popularity. These processes allow for the small-quantity production of complex components that would either be impossible or extremely costly and impractical to fabricate using traditional manufacturing techniques. FFF machines typically build components by laying down successive layers of an extruded material at high temperatures based upon previously designed CAD drawings. Depending on the size and shape of the design file, the 3D printer will vary the size and shape of the layer, creating the desired shape. The high precision of 3D printers allows for non-solid part interiors; they can be fully hollow, fully solid, or somewhere in between, using something known as infill [6]. This infill can be customized in a number of ways, giving printed components interesting structural properties while being only partially solid, saving materials and weight. In small quantities, this process is much more cost-effective than traditional subtractive manufacturing techniques, producing less scrap material while still being able to build high-resolution, complex parts [7].

Despite the many advantages of 3D printing, like other manufacturing methods it has its weaknesses. Although it is possible to manufacture components with very high resolutions (3D printer resolutions range from 50 to 500 microns with the industry standard at 200 microns), The success of a print is mostly dependent on the accuracy of a printer's motors and user calibration. A printer with an advertised 100-micron resolution can easily perform worse due to poor assembly/construction and/or software and calibration. It is also very much an open-loop process; 3D printers are not equipped with the sensors required to read and respond to errors in their printing. The successful manufacture of a part often times is largely dependent on trial and error. This, of course, means that a successful print cannot always be guaranteed, limiting the usefulness of AM in scenarios in which consistently precise components are needed. Without the addition of feedback in the printing process, it is likely that FFF process such as those used by 3D printers will never become more than a prototyping platform.

As NASA continues to move forward in its pursuit of space exploration, its technical needs continue to grow as well, and components of increasing complexity will be required to build its research and exploration devices. The nature of 3D printing lends itself well to the production of these parts, however aerospace parts must be manufactured according to tight

tolerances, and microstructural defects; missed quality standards cannot be tolerated (NIST). Because of its inconsistencies, creating a 3D printed part can be a hit-or-miss which does not make it ideal for one of a kind critical components such as are required on NASA missions. Components of spacecraft and other high value NASA systems must be guaranteed to work every time. If the 3D printing process was able to be characterized, and a sensor set was employed to monitor print parameters in real time, then this problem could be remedied. 3D printing would be transformed from a prototyping platform to something capable of consistently producing end-use components, ready for immediate use both on this planet and beyond.

During this investigation into 3D printer characterization, it was found through experimentation and research that the most common ways in which a 3D print failed were a failure of adhesion and filament feeding issues (RepRap). Of the many potential factors that could cause these issues and of the many possible inputs that could be monitored, three metrics were decided on as a way to begin the characterization of the 3D printing process. A load cell was used to measure the loads of the printed material is deposited, an array of thermometers was used to measure the temperature of the various parts of the printer, and a laser profilometer was used to measure the width of the extruded filament. The proof-of-concept setups used with these sensors allowed for rudimentary data collection from which a set of parameters were created to determine whether or not a print was successful.

1.1 Load Sensing Theory

To ensure the quality and dimensional integrity of a 3D printed component, it is vital that each printed layer adhere to the one before it. The failure of adhesion of successive layers is one of the most common ways in which a 3D print fails. Early detection of this failure would make it possible to ensure a larger percentage of 3D prints are successful. In order to do this, the print bed was placed on top of a load cell which was used to measure force exerted upon it as material is deposited as well as when various motions are executed by the printer head. A graph of load versus time of a successful print would appear as shown in figure 1; as each new layer began, there would be a spike in the force measured as the print head made its initial contact with the previously extruded material. Then, as the layer was built, one would expect to see a gradual increase in the measured force, as more material was deposited onto the print bed. Finally, as the current layer finished and the extruder moved on to the next, the filament strand was stretched and broken off from the rest of the material reel, causing a negative spike in the recorded load as the existing structure was partially pulled away from the print bed. If something were to go wary in the adhesion process, then a different output would be expected, as discussed in section 4.1.

1.2 Thermometer Theory

In-situ monitoring of the 3D printer production process with the use of sensors will enable the manufacturing of high-quality products. The main issue with current 3D printers is the lack of response variables in tracking the production process in real time. The failure of this process can be the result of a variety of factors, including temperature variances in the extruder of a 3D printer and its melt pool, and cooling irregularities due to the ambient room temperature. To monitor temperature variances in the presence of a defect, a temperature sensor was mounted and directed towards the melt pool area, and another was mounted directly behind the extruder. The variations in temperature of the melt pool will be significant to determine deviances from normality from the process signature. This monitoring of temperature will aid in the detection of defects or deviations early on in the printing process to save both time and resources.

Infrared Thermography is a feasible approach to monitoring the temperature by detecting the change in the intensity of the radiation emitted from the point of measurement. This approach was used in the following experiment to measure the melt pool temperature using a noncontact infrared temperature sensor. The results expected from the temperature sensors are variations in the temperature in the presence of a defect or discrepancy. The study conducted with heterogeneous temperature sensors showed a change in temperature of the melt pool in the case of a defective or failed state (Figure 2). The data shows a sharp decline in temperature in the abnormal and failed states. Consequently, this data will be used as a means of comparison with results obtained from the current study. In order to classify and quantify these variations, various temperature profiles were obtained and analyzed for trends.

1.3 Profilometer Theory

The basis of operation of a 3D printer consists of it laying down successive strands of material to form layers, and building up these layers to form three dimensional objects. A simple misplaced or misconstrued strand could easily cause an entire print to fail, and so it is important to monitor this process and catch any errors as soon as possible. To do this, a laser Profilometer was mounted in such a way that allowed it to measure small deviances in the width of a 3D printer's extruded filament. Laser profilometers are typically used to quantify a surface's roughness. They use the principle of laser triangulation to shine a laser at a surface and measure what percentage of light is diffused and/or refracted, and from this information they are able to determine how far away something is from the emitted. The instrument used was extremely precise, having a resolution of one-tenth of a micron. This resolution proved extremely useful for this 3D printer application, as small variance in the width of the filament proved to be telltale signs of printing errors, as discussed in section 4.3.

The data collected from these sensors during a sample print was used to create a set of parameters, which was used to quantitatively determine whether or not a print was successful. Using quantitative measurements such as the ones presented here, future 3D printers will be able to declare a print successful or failed and even correct errors in real time without human interaction or visual inspection.

2. Previous Work

Although a relatively new field of study, several other research groups have also attempted to characterize the 3D printing process. In this section, these past attempts will be summarized with their shortcomings noted.

2.1 Spectral Graph Theory

The spectral graph theory (SGT) study [10] is a novel approach to quantify the dimensional integrity of a 3D printed product for quality comparison purposes. This approach utilizes laser line scans stored in 3D point cloud data to quantify the dimensional integrity of a print. The Fiedler number is derived from the data and used to quantify the dimensional integrity using Cartesian coordinate points. The sampling and analysis methods used in this study were applied to real 3D prints in assessing build quality, and comparing it to the expected specifications. The SGT approach can be implemented in applications where analysis of the dimensional integrity occurs after the product has been printed. The design, thereafter, was altered from the results that show where the defect is most prone to occur. However, the SGT approach fails to monitor the production process in real time, only detecting the defects after the print has occurred. The approach tested in this paper differs in that it attempts to use sensors to monitor the production process in real time, to prevent the defects early on in the production process saving resources and time.

2.2 Heterogeneous Sensors

The study using heterogeneous sensors [11] instituted 15 in situ sensors to monitor the printing production process in real time. The variables being studied include the extruder temperature, melt pool temperature, extruder and table vibration, and table temperature. Various thermocouples, accelerometers, a noncontact IR temperature sensor, and borescope were used to measure the different variables. Statistical analysis of these experimental variables included the calculation of means, standard errors, and confidence intervals. The experiment conducted in this study differs from the one described in the heterogeneous sensors because it uses fewer sensors, and therefore less processing power is required to run and monitor extended prints. The sensors used were different as well. It was found that the optimal number of noncontact IR temperature sensors needed was two. The profilometer was used as another means of measurement to assess build quality by scanning each layer of the print in real time. Furthermore, the data obtained from this experiment was correlated with images and videos obtained from the IR camera to vary data collection platforms. With a variety of data collection methods, thermocouples were used to calculate emissivity values and calibrate the temperature sensors. They were also placed directly on the extruder to correlate and compare data obtained as another means of comparison.

3. Experiment Setup

Modifications were made to a consumer, desktop 3D printer (LulzBot Taz 5) to house each sensor set. Each sensor test was conducted independently, with only one sensor set being mounted and monitored at a time. While future experimentation may warrant the monitoring of the interactions of multiple sensor sets at a time, for this first step, it was important to ensure that no single sensor setup was interacting with and potentially skewing the measurements of any of the others. Several sample CAD drawings were made to gather baseline data sets, the specifics of which are discussed in the following sections. Finally, all prints were made using the Polylactic Acid (PLA) biodegradable polymer [12] with the extruder at 210 °C and the blue painter's-tape-covered print bed at 70°C. To reduce print times and file sizes, as well as make visual analyses of printed components easier, all prints were done using a .4mm layer height. It was found that this setting produced the most consistent prints using the available printer, and were kept constant across all tests to reduce as many anomalies as much as possible. The biodegradable and organic nature of the PLA polymer also served to reduce the carbon footprint of the experimenters as well as limit their exposure to potentially harmful chemicals, especially when compared to other available materials, such as Acrylonitrile Butadiene Styrene (ABS).

The specifics of each sensor setup are discussed in the subsequent sections.

3.1 Load Sensing

3.1.1 Experimental Design

Several CAD files were created to test 3D printer layer adhesion (figure 3). The first two files pictured are simple two-dimensional walls, designed to get a baseline as to what a successful and failed print's mass history might look like. One was printed in the X direction, with the other being printed in the Y direction. Their tapered shape was an intentional design choice made to prevent extraneous mass readings caused by bumps in the print layers. While printing a traditional square wall, at the end of each layer, the filament would often times stretch into a thin string of plastic before fully breaking, causing a buildup of material at one end of the wall. When the print head moved over this buildup as it finished up the next layer, it would push

the entire print into the build plate (and consequently the load monitor), causing a spike in its measured mass. In “real life” three-dimensional structures, the seams of each layer are aligned in such a way that this is not a problem, and so it was determined that these modified two-dimensional structures would still be sufficient examples of what one might encounter when printing traditional three-dimensional structures.

The final CAD file is a simple three-dimensional box, designed to gain an insight into what the mass history of a three-dimensional printed object might look like. To shorten print/trial times and in order to create a simplified data set that better lent itself to analysis, the box was printed without infill and with perimeter widths of one layer. Another step taken towards easier data collection and analysis was to change how far the extruder lifts up in between each layer, known as the Z-lift. By default, the Z-lift is set to zero. In this configuration, a minimal amount of time is spent during the layer change, leading to faster print times, and it is the setting most conventional prints are done with. The delay between a mass change on the load plate and a change in the reading of the load monitor was often times too great, and so it was necessary to slow the printing process down in order to allow the load monitor to adjust to minute changes in mass. To do this, the Z-lift was changed to 10mm. This slowed down each layer change significantly, giving the load monitor enough time to catch the crucial mass spikes during each layer change.

Once it was clear what the mass history of successful adhesion looked like, an adhesion failure test was emulated. To do this, a slip of paper was inserted mid-print in between two of the layers of each of the test prints (figure 4). This emulated an adhesion failure quite well, and as the print head moved from one layer to the next, the layers above the slip of paper peeled up with it. It was determined that a minimum of five trials per configuration were necessary to ensure that the results received were consistent and repeatable, making for a total of 30 trials.

3.1.2 Sensor Setup

It was known that in order to quantify 3D printer layer adhesion, it was necessary to modify a 3D printer to print on top of a load cell (Denver Instruments P-8002D), was used to provide an accurately calibrated load cell and the supporting signal conditioning electronics. To use the balance as a platform for adhesion testing, several configurations were tested. Initially, ABS plastic was simply printed on the load plate of the load monitor, a non-heated surface covered in Kapton tape (figure 5). This produced poor results, as the unpredictable nature of ABS and the fact that it requires a heated print bed led to extremely poor adhesion, preventing even a single layer from sticking to the modified build plate. Even after using a heat gun (Master Appliance HG-301a) to preheat the surface, it cooled down too quickly, causing similar problems. Similar occurrences resulted from using the PLA plastic, this time with the load plate covered in blue painter’s tape (figure 6). Even after preheating the surface with a heat gun, the surface cooled down too quickly, and little to no first-layer-adhesion was achieved. It was then discovered that the heated bed sold with the Tazi 5 printer was removable, and it could simply be placed on top of the load cell (figure 7). This allowed for consistent adhesion. The Z-axis end stop was then modified to set the new, higher bed position as the zero point, rather than the stock configuration.

In order to record the data produced by the load monitor, its RS-232 connection was interfaced with a Windows PC through a LabVIEW program (written by Dr. Godfrey Sauti). Collecting mass measurements every 100 milliseconds, this program then generated a graph of

mass versus time, viewable in real time from the computer's screen and also exported for later viewing and analysis using graphing software (Figure 8).

3.2 Thermometer

3.2.1 Experimental Design

The design of the experiment consisted of the heated printed bed with the blue tape and PLA material, an infrared camera (FLIR T650sc) aimed directly at the melt pool area to capture real time video of the trials, and two type K thermocouples to calibrate the emissivity values of the infrared temperature sensors (Micro Epsilon CT-SF22-C1), (Figures 9 and 10). The thermocouples were placed at the point of measurement for the temperature sensors, and the emissivity values of the sensors were calibrated accordingly to match. The DAQami program was used for the thermocouples. The structure printed for testing was standardized for all the trials. The structure was a 70x5x5 rectangular prism with no infill, and one layer of casing. The mounts for the temperature sensors were designed with the distance: size ratio accounted for. For the CT-SF22-C1 sensors used in this study, the ratio is 22:1. The minimum spot size the sensor can detect the temperature of with a 220mm field of view (distance) is 10 mm. Both sensors were 2.78 cm from the measurement area, so the distance:size ratio was met. There were multiple variations in design for the sensor mounts. The main difference between each variation was the placement and angle of the mount. Designs consisted of mounts that were aimed directly behind, parallel to, and to the side of the extruder. Attempts to measure the melt pool temperature with the sensor consisted of designs that were aimed directly above and from the sides of the point of measurement.

The testing procedure remained constant for both temperature sensors. For each sensor, there were multiple trials of both a successful and a failed print. The resulting temperature was monitored and recorded for each trial using the Compact Connect software. A thermocouple was placed directly on the extruder to monitor temperature consistency and the resulting data was used as a means of comparison to the temperature sensor pointed directly behind the extruder. DAQami was used to record the data from the thermocouple for the duration of the print. For each trial configuration, the IR camera was used to record the printing process, and the resulting data was correlated with the temperature sensor data (Figure 11).

3.2.2 Sensor Setup

To test how temperature variances in a successful build compared to a failed build, two IR temperature sensors, a thermocouple, and an infrared camera were used. A thermocouple was used in conjunction with a data acquisition software (DAQami) to calibrate the temperature sensor, and adjust emissivity values to provide accurate readings. An infrared camera, which has a wider viewing area than the spot sensors, was used to provide visual representations of the temperature throughout the production process, and was correlated with the data obtained from the temperature sensors. Two mounts were designed for the infrared temperature sensors. One mount was angled at a 35-degree angle directly behind the extruder to measure the consistency in temperature for the duration of the print. The second mount was also angled downwards, and was aimed to measure the melt pool temperature as the material was cooling directly (Figure 12). Both sensors attempted to develop patterns and trends in cooling temperatures. This further provided valuable information on how the trends varied in a successful print compared to a failed print. The temperature variances between the two tests that will be conducted will provide a means of comparison to analyze trends.

3.3 Profilometer

3.3.1 Experimental Design

By using a Profilometer, it was possible to detect very small imperfections in a 3D printer's extruded filament. Imperfections, from small ridges to large divots, were detected as sudden variances in the distance measured by the sensor. From that data, it was possible to determine whether or not a print error had been made. To arrive at these conclusions, a very similar procedure to the two preceding sensors was followed. The same simple, hollow box (figure 13) was printed again, however this time, its length was aligned along the Y-axis. This new positioning was to allow the profilometer's laser spot to be able to capture more of the print, as explained in the next section. Similar steps were again taken to emulate a failed print; halfway through, a slip of paper was inserted in between two of the layers (figure 14). This time, however, it was only meant to introduce a ridge into the extruded filament, rather than emulate failed adhesion. Additionally, a second failure case was tested, that being a feeding failure. This was done by releasing the filament feeding latch halfway through the print (figure 15), preventing the printer from extruding filament, as often happens during extruder clogs and other related feeding issues.

Again, five trials were conducted for each test case, making for a total of ten profilometer trials.

3.3.2 Sensor Setup

As shown in figure 16, the mounting hardware of the profilometer consisted of a simple 3D printed bracket along with a number of nuts and bolts. The range of the profilometer (optNCDT 2200-2) two millimeters, 24 millimeters away from the sensor's housing (figure 17). Thus, the sensor was forced to be mounted on the front of the extruder, with the sensor spot approximately three millimeters away from the actual extrusion point. This meant that during parts of the print the sensor was in fact pointing at nothing at all, with the sensor spot outside of its limited two-millimeter range. Despite these limitations, valid data was still able to be collected, and the limited range could even be used to one's advantage, as discussed in section 4.3.

The rest of the setup (figure 18), consisted only of a data conversion device (PC2200-X\USP\IND Convert) that translated the raw signals of the profilometer into an RS-422 interface, as well as providing the sensor with power. The RS-422 interface then went through another converter (Brand), from which a USB COM signal was produced. This was then again interfaced with a Windows PC, running the OEM-provided ILD 2200 tool. The software collected distance measurements every 200 milliseconds, with an accuracy of one-tenth of a micron and no averaging. It also allowed for the real-time viewing of the measured distance, displayed in a constantly-updating graph format. Also like the load monitor setup, this software exported each trial's data in a file format, able to be imported into a graphing software and later analyzed.

4. Data Collection and Analysis

4.1 Load Sensing

The first test was with the X-axis aligned and 2D structure. When the extruder pressed down to start a new layer, it pushed the existing print into the print bed (and consequently the load monitor), causing a sharp increase in the recorded mass. There was a sharp decrease in the recorded mass when the extruder lifted up at the end of each layer (figure 19). This was due to

the filament breaking process, which partially lifted the previously printed material each time. Similar results were seen in the second test, with the Y-axis aligned structure.

The third test was with a 3D structure. It was found that there was an upward spike at the start of a new layer and a downward spike at the end of a layer. However, similar results were achieved even without any filament being extruded (Figure 20). This was due to the scale moving with the print bed, causing the mass measurements to be skewed. The same test was performed with a 2D structure with and without filament. The difference between these two graphs was much less noticeable in comparison with the 3D structure (Figure 21), confirming the notion that these skewed measurements were due to the scale movement. As a result, balance, while being a reasonable approximation to an appropriately mounted load cells for prints with no motion in the bed axis is not suitable when there is significant motion of the bed.

The final test was a print in which failed adhesion was emulated. After three layers, a paper was inserted to simulate a failed adhesion to the next layer. Although the upward spikes at the start of each new layer and the downward spike at the end of each layer continued to be seen, there was a secondary increase in mass at the end of each layer where the paper was inserted, a result of the bulge created by the failed adhesion. As the print head moved over the bulge, it would push the existing print into the load monitor, increasing the recorded mass.

The overall ability to detect errors using the adhesion testing approach as discussed above is plausible. When the failed adhesion tests were compared to the successful tests, there were noticeable differences. (Extraneous mass spikes). However, when applying this concept in real-world applications, factors such as the sensitivity of the load cell, time lag of the device, load monitor surface, and scale movement will have to be taken into account. The sensitivity of the load cell caused several extraneous, unaccounted for data spikes. This may have been from external factors that were difficult to control. For testing purposes, trials with a Z-lift of 10 mm were conducted. This showed a clear pattern in the graphs at the start and end of each layer. However, this consistency in data is not as evident when the extruder is moving at its normal pace. The time lag characteristic of the load monitor may make it difficult to report discrepancies in the product in real time. One critical aspect that may have also caused a skew in our data was due to the leveling of the load monitor. Although the print bed was leveled, the table was not. The movement of the scale may have also caused inaccurate readings for the 3D structure tests. When the results with and without filament were compared to the X and Y-axis aligned tests with and without filament, there was a noticeable difference, however the same was not true for the 3D structure tests, which showed the same results with and without filament being extruded. Because the 2D structure tests had the extruder move in only one direction, the scale movements were caused fewer skewed measurements. It is crucial that these factors get accounted for to ensure accurate results from the load monitor.

A proposed set of parameters that will be beneficial in implementing the adhesion monitoring in a 3D printer are as follows. The bed will need to be leveled. The load cell will be zeroed depending on the print bed design being used. Once the load monitor is connected to a data collection program, weight differences will be recorded for the duration of the print. Weight ranges for a successful print will need to be calculated beforehand to detect a failure of adhesion. Depending on the design, this may differ.

4.2 Thermometer

Temperature sensor 1 is pointed downward at a 35-degree angle directly behind the extruder. Temperature sensor 2 is angled directly towards the melt pool area. The data collection

period was two minutes, 52 seconds. Data was collected every 100 milliseconds for both tests. Results from sensor 1 were consistent throughout both the failed and successful tests (Figure 22). The reason for this consistency was due to the measurement spot of the sensor. There is no expected change in the temperature directly behind the extruder, regardless of a defect. The characteristic peak and dip as seen in the graph (figure 23) is due to the movement of the extruder in the rectangular prism. The peak is the result of measuring directly after the filament has been extruded, whereas the dip is a measurement of temperature after the filament has been cooling for a short period of time. This graph pattern will not be consistent for every printed design. However, when compared to the failed test of the same design (figure 24), there was no significant difference in results. The failed test graphs had similar shapes with characteristic successive peaks and dips.

When compared to sensor 2, the graphs looked noticeably different. Sensor 2 was measuring the melt pool temperature directly as the filament was being extruded. The successful trial graphs had the same shape as sensor 1 with characteristic peaks and dips (figure 25). However, the failed test trials had, on average, lower temperatures overall compared to the successful tests. Furthermore, the graph shape changed to include larger spikes downwards after the paper was inserted (Figure 26). The lower temperatures are due to the failure of the layers adhering to each other effectively. The product is printed on a heated bed and when each successive layer adheres to the one before it, the layer is already heated. However, once the paper is inserted, it is no longer heated causing the layers to deform and a change in temperature. 99% confidence intervals were conducted for both sensor 1 and 2. For sensor 1, it can be estimated with 99% confidence that the interval ranging from 71.3207 to 71.4234 captures the true mean temperature of the successful print. For sensor 2, the same can be estimated with the interval ranging from 64.0794 to 64.4370. Once the value ranges outside these intervals, it can be said that there may be a defect in the production process assuming all the parameters are the same as this experiment. These values may differ due to different printed products, and variations in experimental design. The thermocouple data was also compared to the successful print graphs for both sensors. The thermocouple graph showed the same peaks, dips, and large variation in temperature (Figure 27).

The large variations in the resulting graphs can be attributed to the ambient temperature conditions and other uncontrolled variables. Consequently, it is important to use both sensors. Although sensor 2 gives the most information regarding the defects and discrepancies, both are needed to account for the variation in data seen in both graphs. The results obtained from this experiment were similar to those in the heterogeneous sensors study. The graphs had characteristics peaks and dips and a large variation. Furthermore, the temperature dropped significantly in the presence of a defect and failed print.

From these results, it can be concluded that it would be most beneficial to monitor the melt pool temperature for detection of defects and discrepancies. Although sensor 1 provided details on a plausible temperature range, sensor 2 provided a temperature range to detect defects. In the future, temperature sensors and thermocouples can be used to detect defects on the basis of temperature variations in the melt pool. If the temperature does not fall in the specified range, then it can be denoted as a defect. A combination of sensors is needed to obtain plausible values for temperature ranges. A proposed set of parameters to implement the IR temperature sensors in a 3D printer in the future is as follows. The distance: size ratio of each sensor will need to be calibrated depending on how fair the edge of the sensor is from the measurement point. Thermocouples will be used to calculate the emissivity values and calibrate the temperature

sensors accordingly. Since each object emits a different amount of radiation, this step will be critical in obtaining accurate temperature readings. The temperature sensors will be connected to the Compact Connect data collection program to take temperature readings for every specified time interval. An IR camera can be used as another means of temperature calibration and to provide visual representations of the temperature variations for the duration of the print. The resulting data can be analyzed and subsequent ranges of temperature values can be calculated on the basis of the design being printed. The values will differ for each design, consequently, a preliminary test will need to be performed to determine these parameters.

4.3 Profilometer

As shown in figure 28, each trial lasted approximately 3 minutes (180 seconds), and each successful trial is primarily characterized by a repeating pattern of flat lines of varying heights with gaps in between. This data is easily confused at first glance, however it is important to note that any time the laser spot went out of range, the software would automatically return a null value of -10mm. In the graphs shown, these Y-values were cut off, showing a Y-axis range of .5mm to 2mm (the full range of the sensor is 0mm to 2mm, however for easier viewing that range has been reduced somewhat). This cropping produces the “floating” flat lines shown. When reading the graphs, one must also keep in mind the shape that was being printed; an oblong rectangle. Because the Profilometer laser spot trailed the print head by approximately 3mm, it was only able to “hit” the extruded filament on straight Y-axis moves. Whenever one of the shorts end was being printed, the extruded filament would temporarily move out of range, producing a null value of -10mm. As soon as the opposite wall of the rectangle moved back in range, the software would again begin outputting values as the extruder moved along the Y-axis, this time in the opposite direction.

This is also the reason behind the different line heights; during the first Y-axis move, the profilometer was measuring freshly extruded filament, trailing the extruder directly. During the second Y-axis move, it was measuring the previously extruded layer, preceding the extruder. The previous layer always going to be slightly farther away, anywhere from 1.7mm to 1.9mm away from the sensor, while the freshly extruded layer was naturally going to be closer to the sensor, around 1.1mm to 1.3mm away. This difference of course makes sense, as each layer was .4mm high, and one would expect to see such a difference in between a freshly extruded layer and the one that came before it.

During each successful-print trial, it is important to note the relative stability of each of the flat lines. None of them range greater than .2mm from their average, and most of the deviations shown are due to vibrations in the print head, where the sensor was mounted. When looking at a trial in which a ridge was introduced using a slip of paper (figure 29), it is easy to see exactly where and when this anomaly occurred. Each time the profilometer passes over the point of insertion, the ridge, being closer to the sensor’s emitter, creates a downwards spike in the distance versus time graph. Exactly how large this dip is varying from trial to trial, however it is easy to see a very drastic change in the average slope of the line. It is interesting to note that as subsequent layers are deposited over the point of insertion, the spikes tend to become less and less pronounced; this, of course, is due to the PLA plastic’s forgiving and flexible nature, as it is able to fill in smaller gaps and ridges.

Quite a different story can be told about the feeding failure trials, however (figure 30). Almost as soon as the filament latch was released, the extruded filament moved out of range of the profilometer and a null value of -10mm was returned. This null value continued to be

exported, unchanging, until the end of the print. It is for this reason that filament feeding issues were perhaps the easiest and most reliable to detect; as the filament remained “jammed,” the printer would simply continue on its upward tract, performing all the correct movements for each layer while not actually extruding any filament. As it moved upward, the profilometer would simply be moved farther and farther out of range, continuously returning a null value. It is for this reason that a fairly range-limited profilometer might actually be useful, as stated earlier.

Were a profilometer of some sorts to be fully implemented into a closed-loop 3D printer, it is reasonable to expect that a set of parameters would have to be designed to determine whether or not a given print was successful. One such example of these are as follows:

Upon the initial construction of said 3D printer, a set of calibrations would have to be run to determine where in the sensor’s range freshly extruded filament would fall (in this example it was between 1.1mm and 1.3mm into the sensor’s range, however depending on the specific configuration this be any number of possible values). The same would have to be done for moving in the other direction, this time for all possible layer heights (one could also simply assume this distance to be the layer height added to the previous calibration value, however as seen in the data presented a range of factors, from sensor vibration to sensor accuracy, can invalidate such assumptions). Following these steps, a highly customized set of G-Code¹ and/or a software suite must be run on the 3D printer, a computer, or both, that interprets the profilometer data at specific points to ensure that the proper print quality has been achieved. These specific points at would be times during which the software was aware that the extruded filament was in range. It would take into account the specific mounting of the profilometer and how far it trailed the extruder (hopefully the trailing distance would be less than 3mm, however without additional sensors it would be impossible to monitor the extruded filament from all sides and during all extruder movements) and from those specifications take sample measurements of the print. It would be during these sample measurements that any anomalies would be detected. If it were to constantly monitor the profilometer data, then it is likely that the majority the received data would be the previously-described null values, leading to false positives.

A fully closed-loop 3D printing system might have any combination of these previously described sensors, as well as others not explored during this work. This sort of system would likely be controlled by a highly specialized suite of software, designed to interpret many different sensors concurrently, allowing it to accurately determine the state of its print. During this proposed device’s print, if a sensor were to detect something classified as an error (unexpected ridge, adhesion failure, feeding failure, improper melt pool temperature), then it would record the nature of that error before continuing on. After a predetermined quota of errors had been reached, the print would be declared failed and abandoned. Although many would likely be disappointed in returning to a print only to find that it had been abandoned, it would be far less wasteful than simply continuing to build a component that will be discarded regardless. A fully closed-loop system might even be able to notify a user of a part failure, whether it was through a simple visual indicator, such as a light emitting diode (LED), or via something as complicated as a smartphone indicator.

¹ Although there are a huge number of variants, G-Code is the name for the language most commonly used by computer numerical control (CNC) devices.

5. Future Directions

Characterizing the 3D printing process was a multi-faceted process that took many different steps. Three different sensor arrays; a load cell, IR thermometers, and a profilometer were mounted to a desktop 3D printer to measure layer adhesion, printer temperatures, and the thickness of the extruded filament. According to the data shown and the conclusions drawn from that data, it is safe to say that any one of these sensor arrays or arrangement of sensors would be a viable way to characterize the 3D printing process. Using the data presented parameters described, it would be possible to at some point create a fully closed-loop 3D printing system. Because of these facts, this first foray into 3D printer characterization was a success.

As briefly described earlier, the end goal of this work is to create a fully closed-loop 3D printing system. This proposed system would have a whole suite of sensors; all being used to inform the 3D printer of the exact nature of its print. Although what was earlier proposed would simply cancel a build upon detecting too many errors, the final solutions would in fact be able to modify its print parameters (extruder/bed temperature, printing speed, etc.) in real time. Such actions would allow for a higher success rate, as small errors could be accounted for and the overall quality of the print would be preserved. The current state of 3D printing requires users to spend what can sometimes amount to days troubleshooting, settings tweaking, and trial and error before a component of sufficient quality is achieved. The amount of time and materials wasted doing such things are often unaffordable by many, with NASA's limited budget as a chief example.

These experiments are an initial step into 3D printing characterization; there is a long way to go before reaching the proposed goal. Although it is possible to mount all the sensors onto the 3D printer at once, no long-term testing has been conducted on the wear and tear these modifications might have on the control motors and linkages. This is not to mention the fact that the sensors make it difficult to access and repair certain parts of the printer (the profilometer and load cell bed chief among them). Sensor placement is also something that needs a great deal of exploration; given the time restraints of this work, it was only possible to test a single configuration of each of the sensors, based off of some previous research and educated guesses. The profilometer is a great example of this - it is very possible that a different placement/trailing distance would have greatly changed the measurements received. Different types of sensors may also have produced different, if not conflicting, results; so little research has been conducted on this matter that it is hard to say what the "best" sensor array is.

Hardware limitations aside, the main challenge in reaching the end goal would be a matter of software. Each test was conducted using a different piece of software, with the main output being a simple line graph. A fully-integrated solution would have to interface each of the sensors using a unified protocol that would allow it to accurately and efficiently assess the state of each sensor and make decisions based upon these inputs. It would have to run on a platform capable of controlling a 3D printer, whether that be a full desktop computer or an embedded single board computer (SBC). The SBC or desktop would have to be capable of running this software, without getting too bogged down or overheating. The list goes on and on; ultimately, the full process may take up to several years to complete, however this was an important first step towards realizing that goal.

Despite the many roadblocks in the way, this proof-of-concept project proves that 3D print characterization is possible. Hopefully, this work will be used to realize such goals, and NASA, as well as others, will be able to use 3D printers for more than basic prototyping. At

some point, an aerospace engineer may be able to design a component using CAD one day, and the next day have it flying into space, ready to explore the universe.

Acknowledgements

Dr. Godfrey Sauti, mentor, identified the task needed to be investigated and defined the parameters of the experiment that was conducted. He also provided us with a program in LabView for the detection of weight changes in the adhesion testing. Mr. Christopher Stelter, a NASA researcher, helped in the research and design process by providing helpful suggestions on sensor placement. Ms. Becky Jaramillo helped by recommending us to work with Dr. Sauti. Ms. Becky Jaramillo also worked with Dr. Margee Greenfield to organize the Governor's School Engineering program in which we had the wonderful opportunity to work alongside with NASA researchers and interns in the Materials Science Laboratory. They also helped in the technical writing and presentation process.

Figures

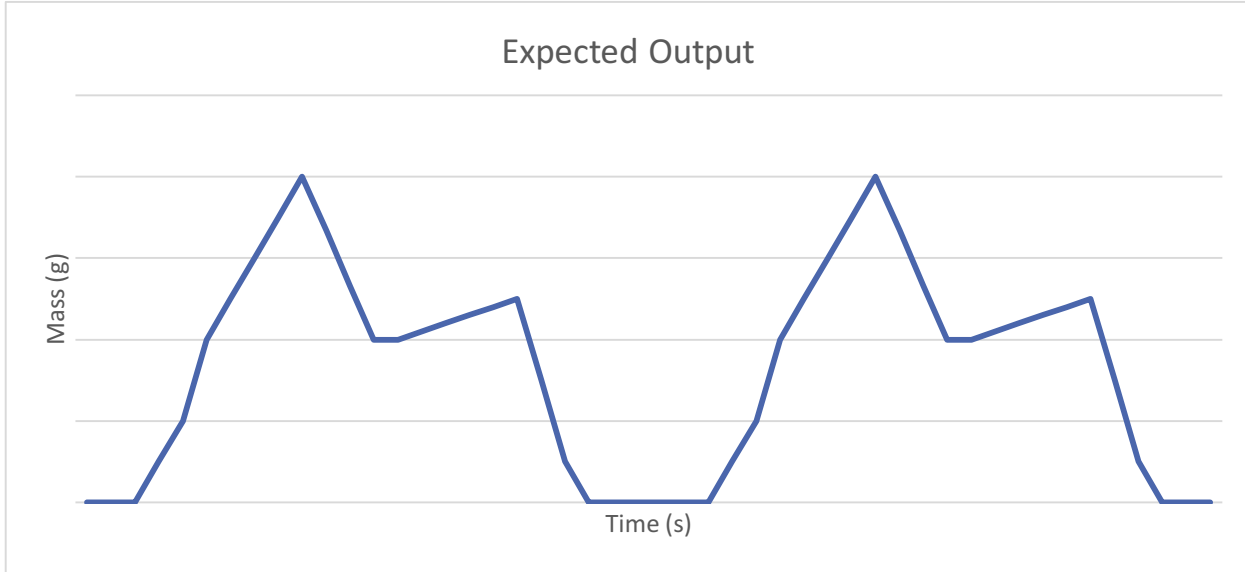


Figure 1: The expected mass history of the load monitor

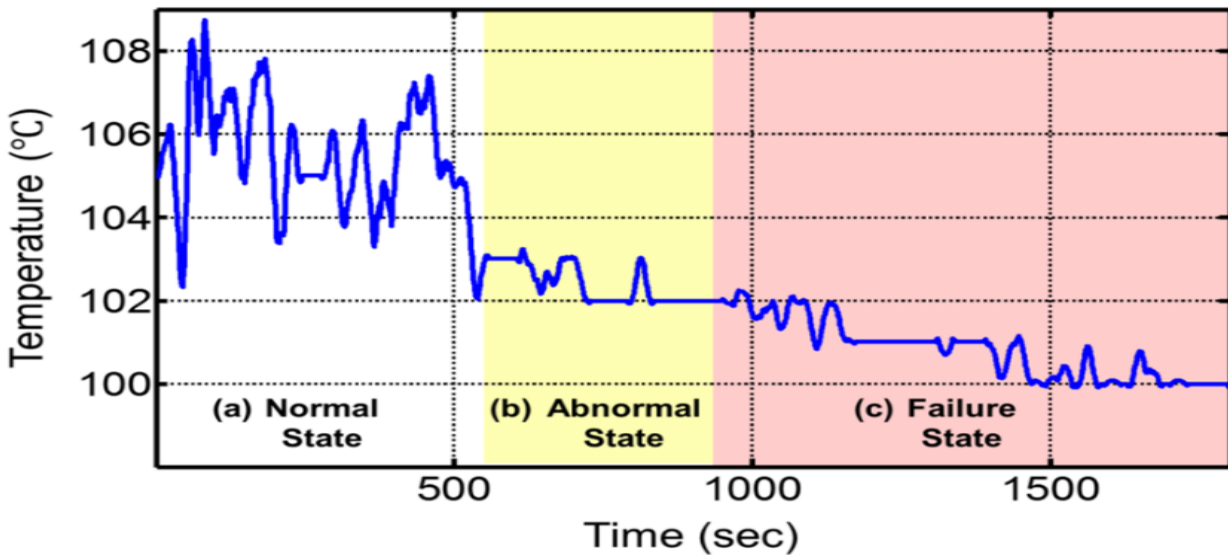


Figure 2: Expected outcomes based on previous studies done on melt pool temperature variations.

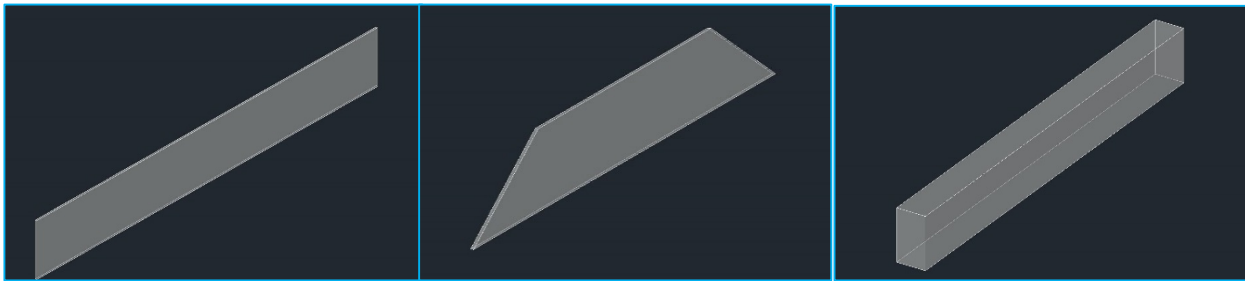


Figure 3: The CAD files used for the adhesion test. From left to right: square wall, tapered wall, 3D rectangle.



Figure 4: A slip of paper inserted between two of layers, designed to emulate an adhesion failure.



Figure 5: The first attempted print surface.



Figure 6: The second attempt; PLA plastic on a blue painter's tape-covered load plate.



Figure 7: The final, successful print surface; the stock heated bed placed directly on the load cell.

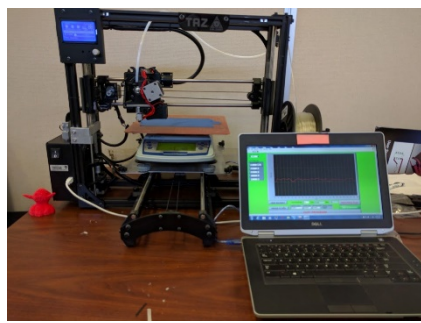


Figure 8: The experimental setup of the adhesion test.

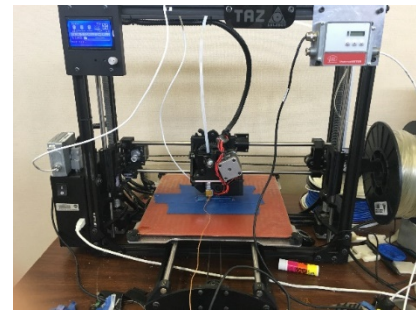


Figure 9: The experimental setup of the thermometer test.

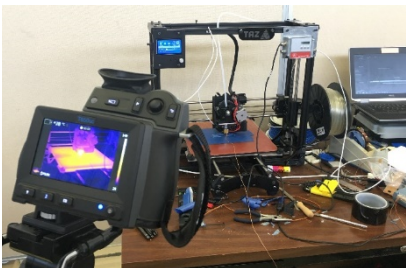


Figure 10: Experimental setup with infrared camera

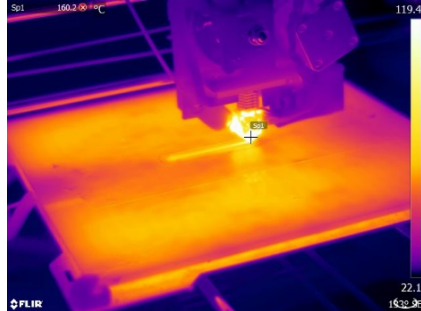


Figure 11: Data correlation with IR camera



Figure 12: Finalized sensor placement

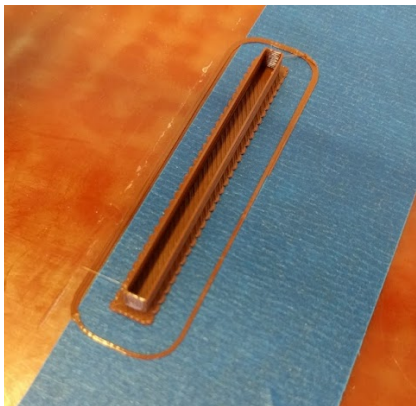


Figure 13: The 3D structure used in the profilometer test.



Figure 14: An inserted piece of paper to add a defect to the print.

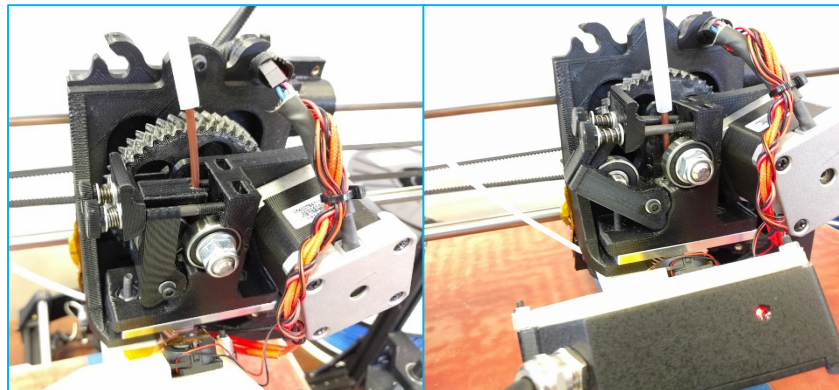


Figure 15: The feeding latch was released halfway through to emulate a feeding failure.

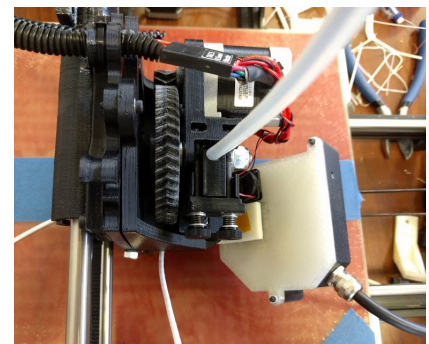


Figure 16: The 3D printed profilometer mount.

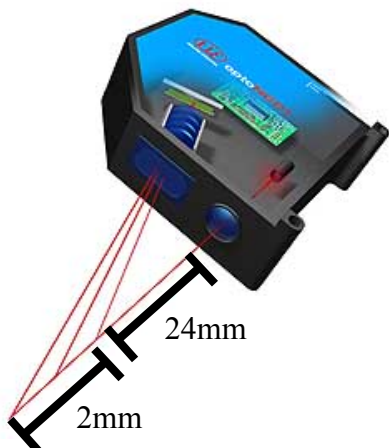


Figure 17: The limited 2mm range of the profilometer.

Image: Xpertgate.de

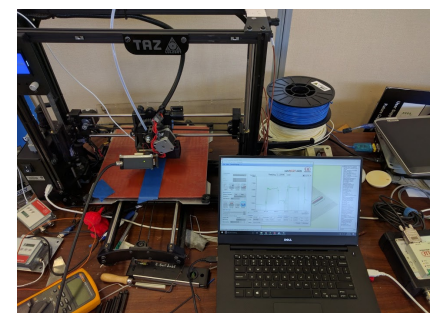


Figure 18: The experimental setup of the profilometer test.

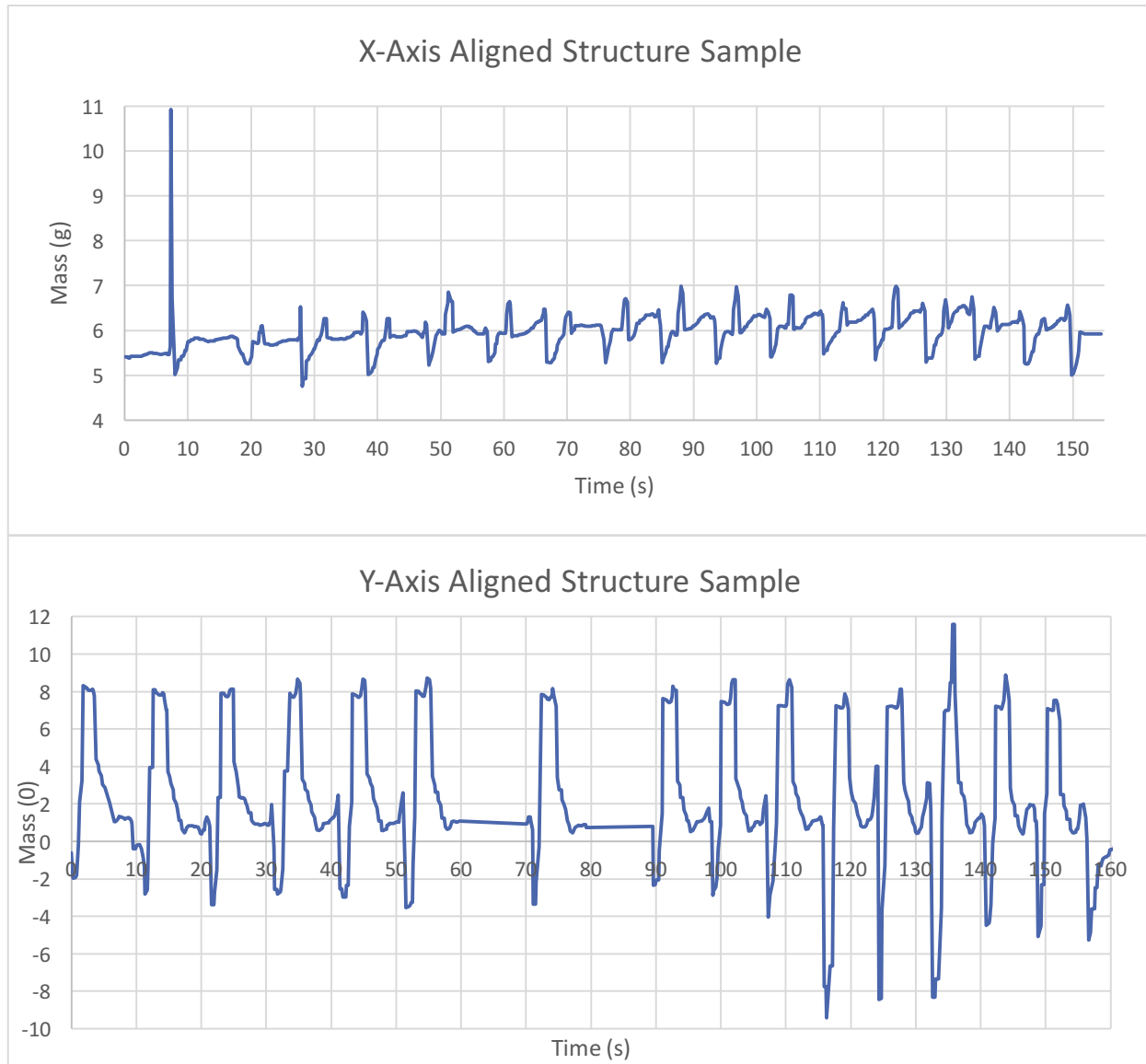


Figure 19: Sample mass histories of X and Y-axis aligned test

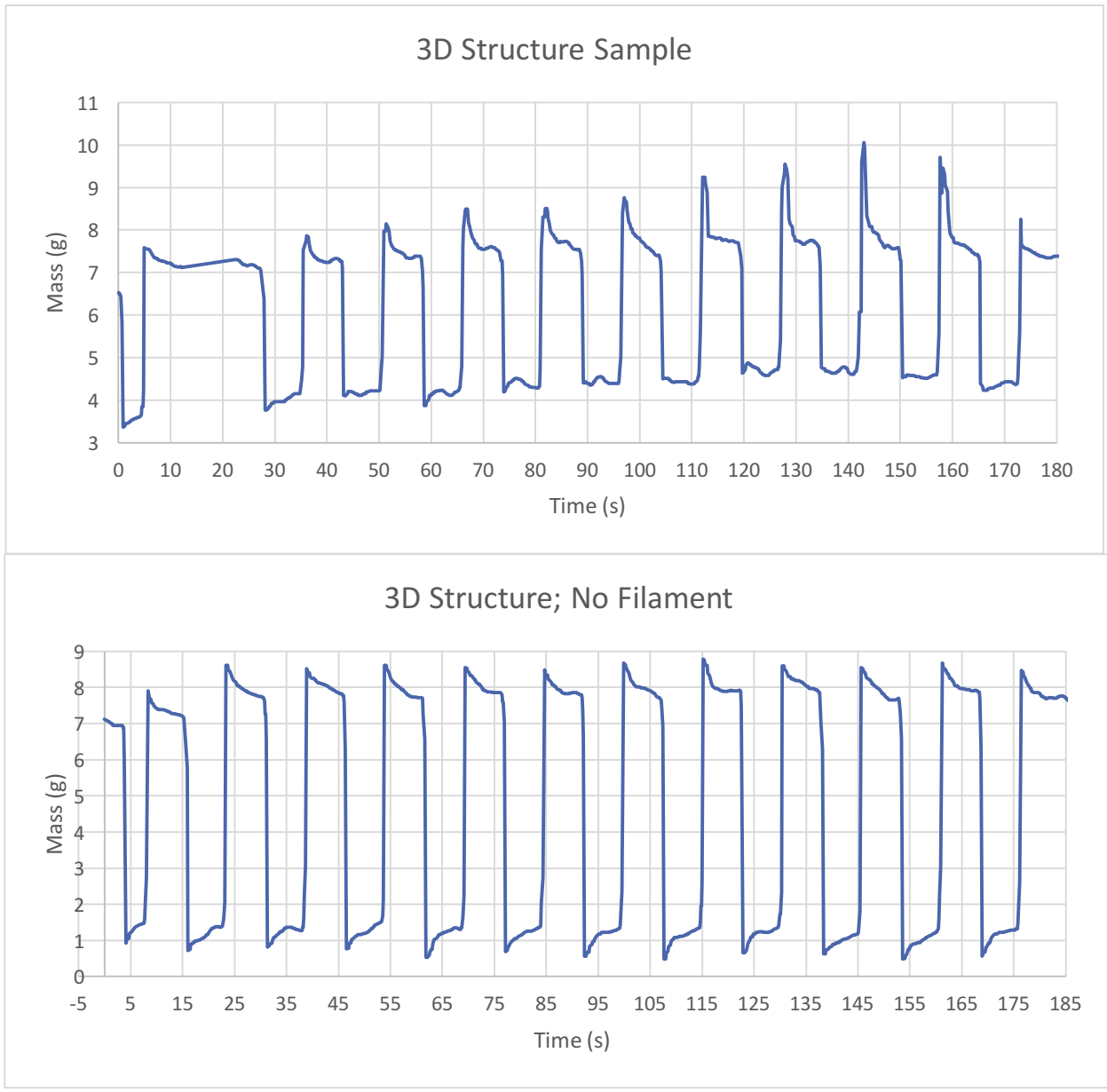


Figure 20: The mass history of the 3D structure with filament (left) and the mass history of the 3D structure without filament (right). There is very little perceptible difference between the two.

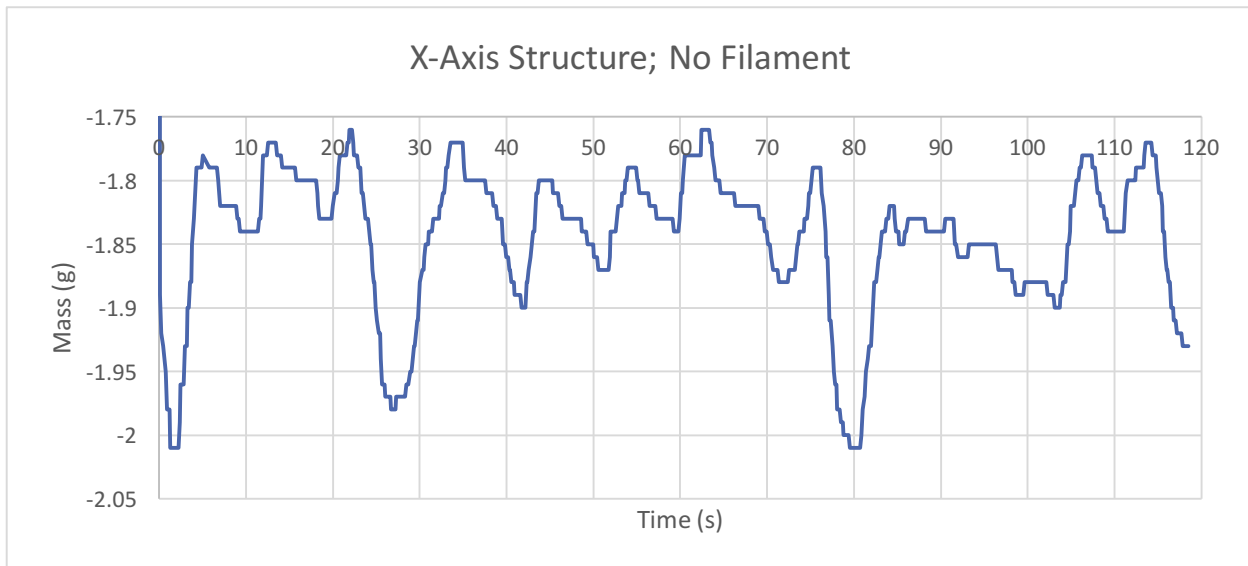


Figure 21: The mass history of the X-axis aligned structure was very different without filament.

Descriptive Statistics: TAct

Statistics

| Variable | N | Mean | StDev | Minimum | Q1 | Median | Q3 | Maximum |
|----------|------|---------|---------|---------|---------|---------|---------|---------|
| TAct | 5175 | 71.3721 | 1.43399 | 68.3000 | 70.3000 | 71.2000 | 72.3000 | 77.2000 |

Descriptive Statistics: TActFail

Statistics

| Variable | N | Mean | StDev | Minimum | Q1 | Median | Q3 | Maximum |
|----------|------|---------|---------|---------|---------|---------|---------|---------|
| TActFail | 5138 | 70.1240 | 1.87352 | 60.3000 | 68.2000 | 70.7000 | 71.4000 | 74.5000 |

Figure 22: Sensor 1. Results fairly similar for successful and failed trails

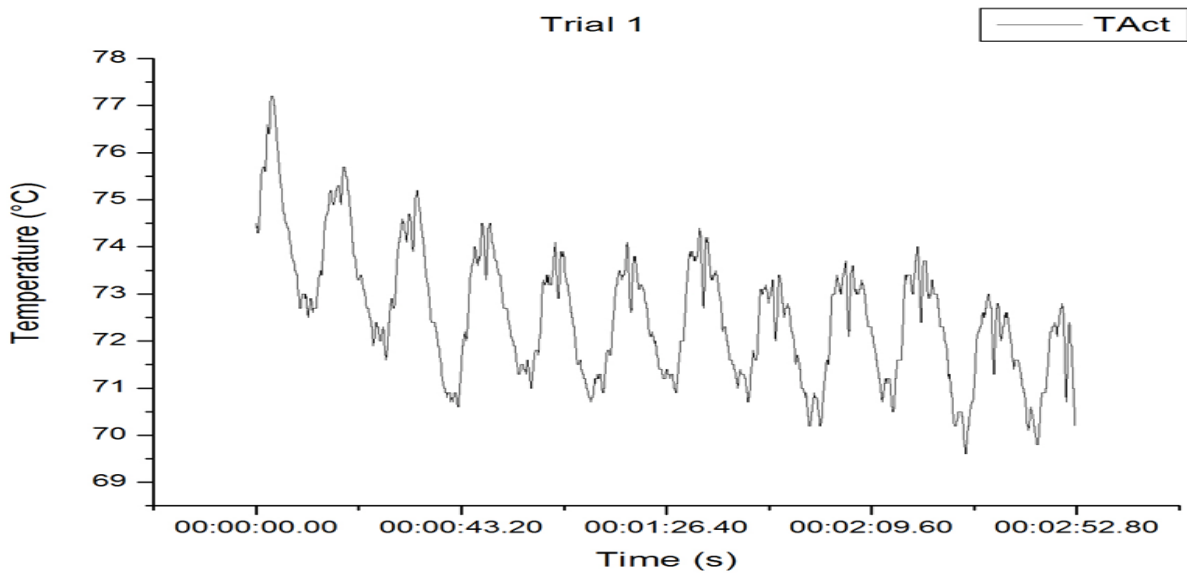


Figure 23: Sensor 1 successful trial. Characteristic variation in temperature with successive peaks and dips

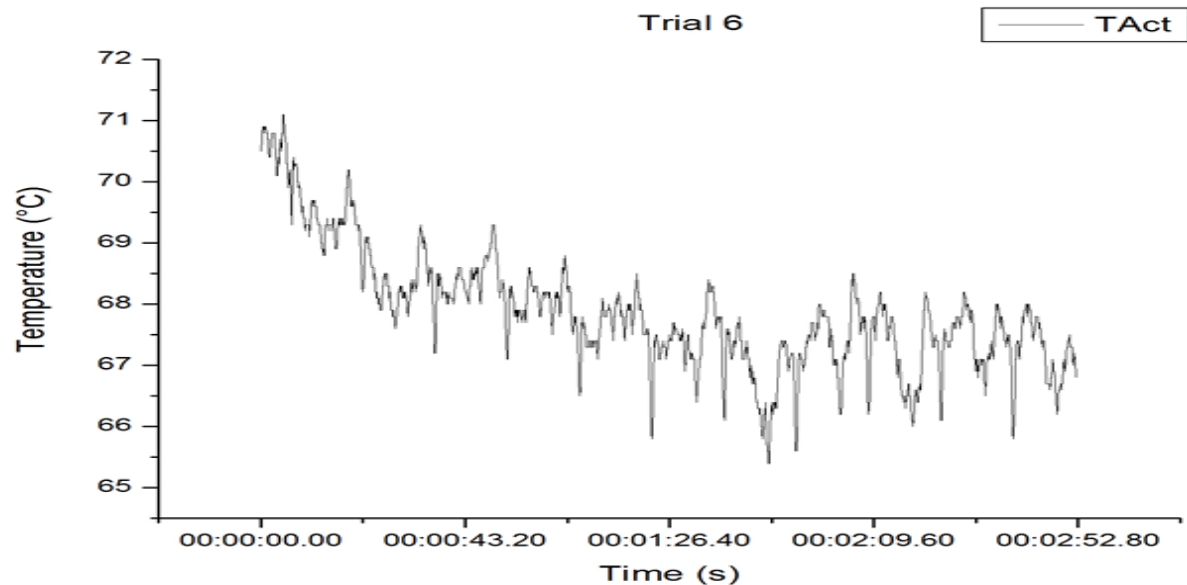


Figure 24: Sensor 1 failed trial. Characteristic variation in temperature with successive peaks and dips

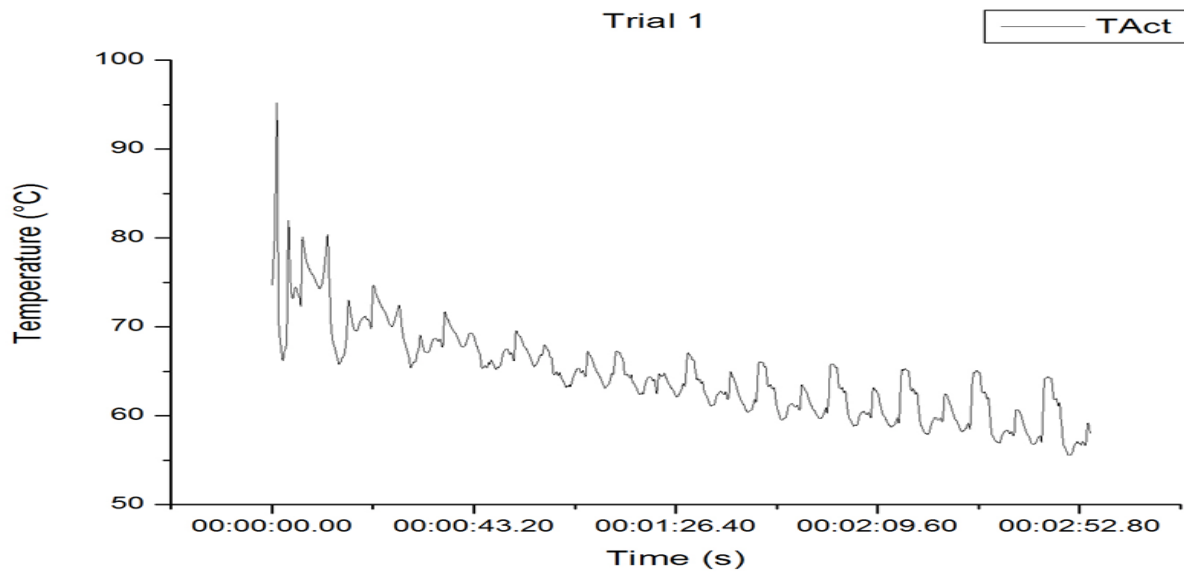


Figure 25: Sensor 2 successful trial. Results similar to sensor 1 with characteristic peaks and dips.

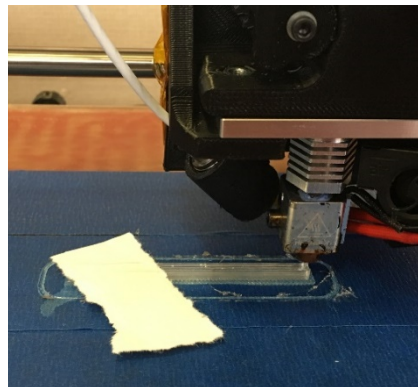


Figure 26: Failed adhesion simulation

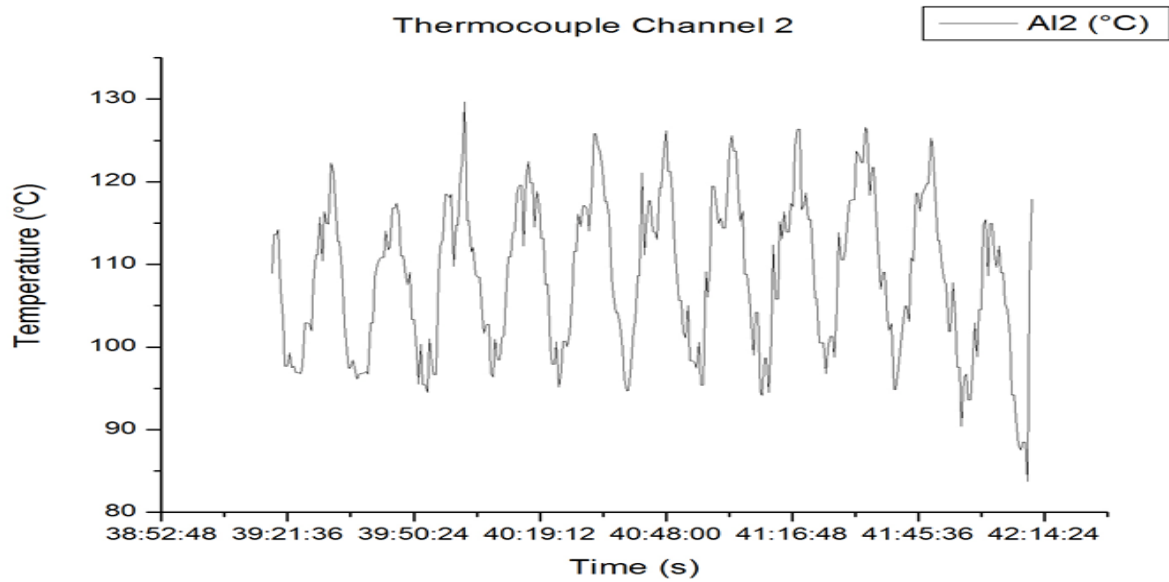


Figure 27: Thermocouple graph with similar characteristic peaks and dips as sensor 1 and 2.

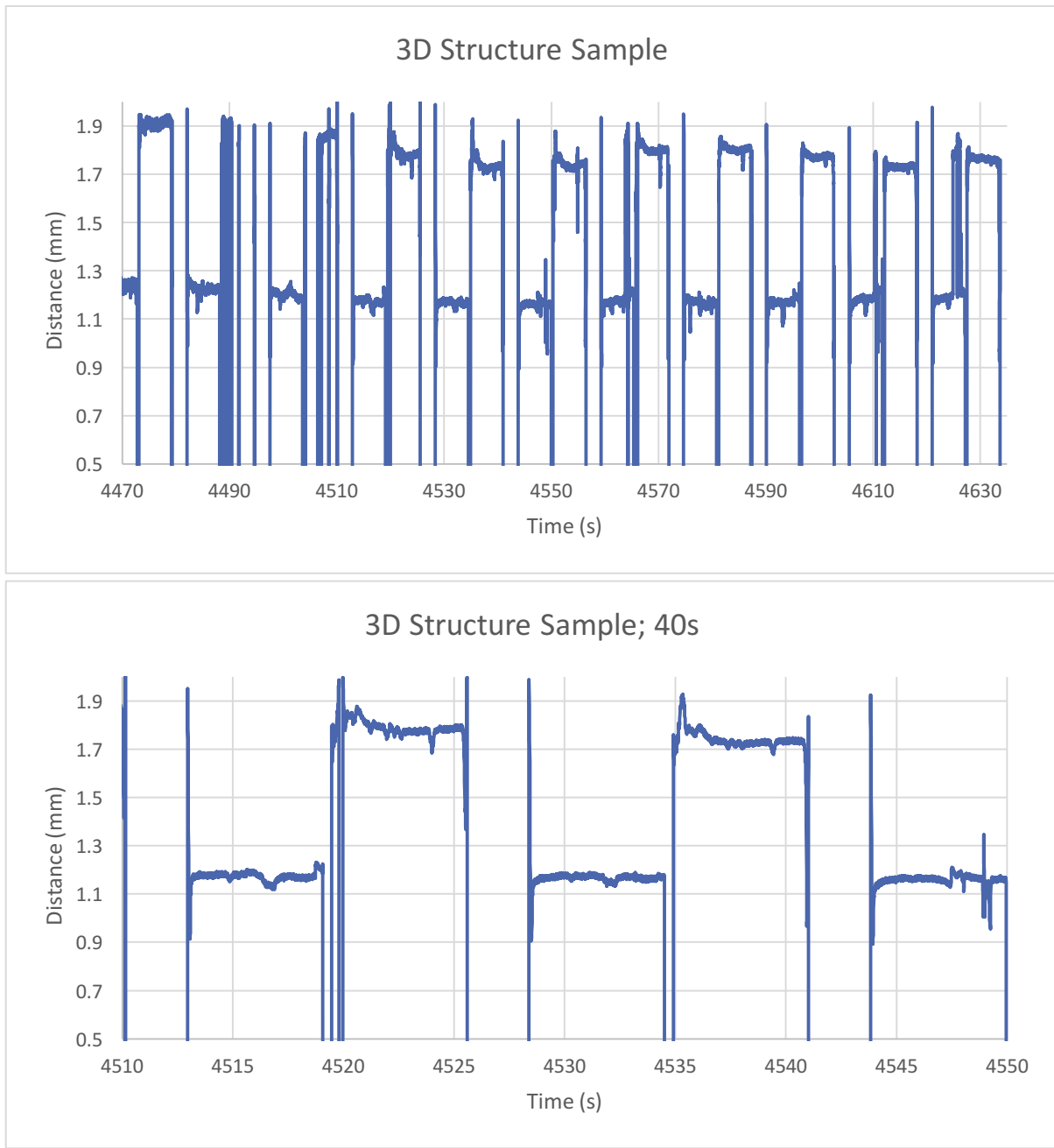


Figure 28: A successful distance history as measured by the profilometer. A 40 second, “zoomed in” excerpt is shown on the right.

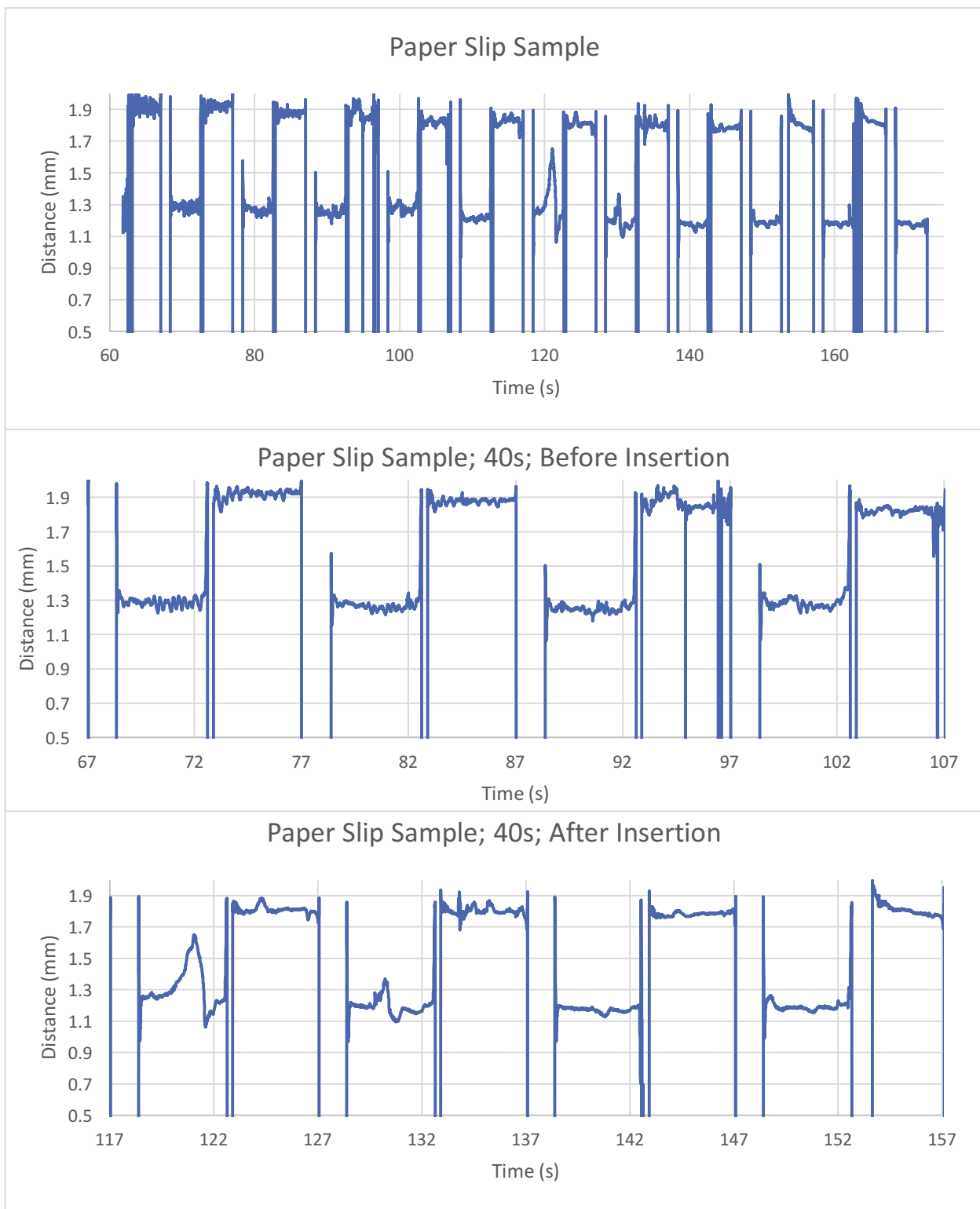


Figure 29: A distance history of a failed print. The rightmost graphs are “zoomed in,” 40 second excerpts of the full trial, to the left.

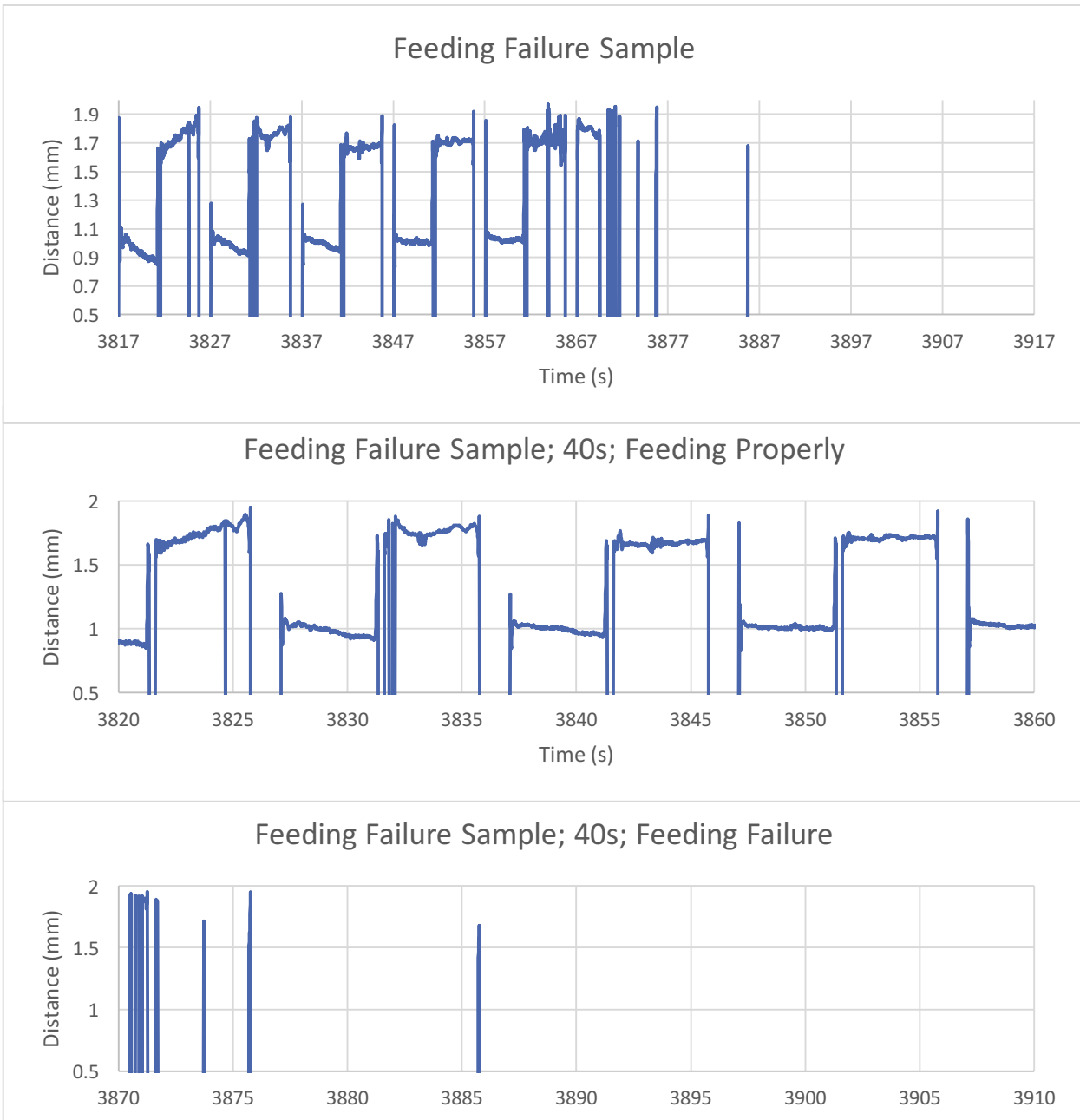


Figure 30: A sample distance history of a failed print. The rightmost graphs are “zoomed in,” 40 second excerpts of the full trial, to the left.

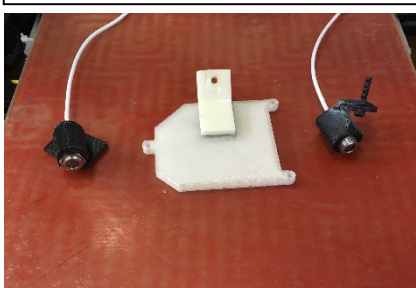


Figure 31: The final 3D printed sensor mounts

Works Cited

- [1] Additive Manufacturing, Laser-Sintering and industrial 3D printing - Benefits and Functional Principle . (n.d.). Retrieved July 22, 2016, from
http://www.eos.info/additive_manufacturing/for_technology_interested
- [2] Cooper, K. P. (2012). Direct Digital Additive Manufacturing and Cyber-Enabled Manufacturing Systems. *ASME/ISCIE 2012 International Symposium on Flexible Automation*. doi:10.1115/isfa2012-7269
- [3] Discenzo, F. M., Pai, R., & Carnahan, D. (2010). National workshop on challenges to innovation in advanced manufactruing-industry drivers and R&D needs :. doi:10.6028/nist.ir.7723
- [4] Donmez, A., Feng, S., Fesperman, R., Lane, B., & Mani, M. (n.d.). Real-Time Control of Additive Manufacturing Processes. Retrieved July 22, 2016, from
<http://www.nist.gov/el/isd/sbm/rtcam.cfm>
- [5] Embedding sensors during additive manufacturing | Lloyd's Register. (n.d.). Retrieved July 22, 2016, from <http://www.lr.org/en/services/additive-manufacturing/research-and-resources/embedding-sensors-during-additive-manufacturing.aspx>
- [6] Feeny, D. (2013, August 29). FFF vs. SLA vs. SLS - 3D Printing. Retrieved July 22, 2016, from <http://www.sd3d.com/fff-vs-sla-vs-sls/>
- [7] Hopkinson, N., & Dickens, P. (2013, August 29). FFF vs. SLA vs. SLS - 3D Printing. Retrieved July 22, 2016, from <http://www.sd3d.com/fff-vs-sla-vs-sls/>
- [8] Kremer, K. (2016, February 12). Obama Administration Proposes Smaller 2017 NASA Budget of \$19 Billion with Big Exploration Cuts - Universe Today. Retrieved July 22, 2016, from <http://www.universetoday.com/127309/nasa-2017-budget/>

- [9] LaMonica, M. (2013, April 23). Additive Manufacturing. Retrieved July 22, 2016, from
<https://www.technologyreview.com/s/513716/additive-manufacturing/>
- [10] Rao, P. K., Liu, J. (., Roberson, D., Kong, Z. (., & Williams, C. (2015). Online Real-Time Quality Monitoring in Additive Manufacturing Processes Using Heterogeneous Sensors. *Journal of Manufacturing Science and Engineering J. Manuf. Sci. Eng.*, 137(6), 061007. doi:10.1115/1.4029823
- [11] Rao, P., Liu, J., Roberson, D., Kong, Z., & Williams, C. (2015). Online Real-Time Quality Monitoring in Additive Manufacturing Processes Using Heterogeneous Sensors. *Manufacturing and Engineering Science*, 137. Retrieved July 22, 2016.
- [12] Rogers, T. (n.d.). Everything You Need To Know About Polylactic Acid (PLA). Retrieved July 22, 2016, from <https://www.creativemechanisms.com/blog/learn-about-polylactic-acid-pla-prototypes>